SAND2014-19627C

Effect of Relative Humidity on Corrosion of Steel under Acidified Artificial Seawater Particles

Eric J. Schindelholz
Sandia National Laboratories
Albuquerque, NM, 87123

Bailey E. Risteen
Chemical and Biomolecular Engineering
Georgia Institute of Technology
Atlanta, GA 30332

Robert. G. Kelly
Materials Science and Engineering
University of Virginia
Charlottesville, VA 22902

ABSTRACT

The aim of this work was to elucidate the relationship between the hygroscopic behavior of acidified artificial seawater (ASW) microparticles, as a proxy for sea salt aerosol (SSA), and the atmospheric corrosion of mild steel contaminated with them. The wetting and drying behavior of acidified ASW microparticles deposited on an inert interdigitated electrode sensor was characterized by impedance measurements. Carbon steel coupons loaded with the same contaminant were subjected to isohumidity exposures for up to 30 days. The resulting damage was quantified by optical profilometry. Sustained corrosion was detectable down to 11% RH, with significant admittance of ASW deposits on the sensor at <2% RH after 24 h, likely due to the presence of trapped electrolyte. Trends in corrosion loss versus RH were not directly reflective of the major liquid-solid phase transitions observed for particles on the sensor. The results bring into question whether SSA-contaminated surfaces ever dry with regard to corrosion being possible in ambient outdoor environments.

Keywords: atmospheric corrosion, deliquescence, time of wetness, sea salt, sodium chloride, aerosol

INTRODUCTION

While it is obvious that for corrosion to occur under atmospheric conditions, sufficient electrolyte must be present to support electrochemical reactions, it is not obvious what the minimum environmental conditions are that create sufficient electrolyte. One key environmental condition is relative humidity (RH), which is a measure of water activity, and another is the state of the surface, which is commonly contaminated by hygroscopic atmospheric contaminants (i.e., soluble salts). By definition, one could expect that some amount of water would be present on a surface exposed to an atmosphere above 0% RH. The presence of water alone, however, is a necessary but not sufficient condition for corrosion to occur. It must also be present in adequate amounts to solvate and conduct ions. Time of wetness (TOW) is an attempt to quantitatively characterize the fraction of time during which this occurs. Thus, it is important to quantitatively understand the relationship between relative humidity, the hygroscopic behavior of relevant soluble salts, and the corrosion response of the material of interest.

Corrosion in atmospheric marine environments is generally driven by the deposition of sea salt aerosol (SSA). This type of aerosol is not only capable of breaking down passive films of many alloy systems, but also, because it is highly hygroscopic, of extending the duration in which exposed surfaces remain wet and corrosion possible (i.e., time of wetness). Measurements of surface wetness using electrode-based wetness sensors at outdoor marine sites, where sea salt particles are the primary contaminant, indicate that TOW can approach unity - almost never dry - even down to low humidity levels.[1,2] The persistence of significant conductance to such low humidity levels is often attributed to the presence of magnesium chloride salts, such as $MgCl_2.6H_2O$ (carnalite), which has a deliquescence relative humidity (DRH) of 33% at room temperature.[3-5] The DRH of a salt is the humidity above which it spontaneously

absorbs water to form a bulk electrolyte (solid-aqueous phase transition). Indeed, given its DRH and that Mg^{2+} is the third most populous ion in sea salt following Na^{+} and Cl^{-}, electrolyte rich in Mg^{2+} and Cl^{-} is often viewed as the active component of SSA with regard to low humidity corrosion. Additionally, the DRH of $MgCl_2.6H_2O$ is commonly taken as the threshold between wet and dry surfaces contaminated with sea salt.[1,6]

In our previous work, we examined the relationship between relative humidity, the hygroscopic behavior of SSA proxies composed of NaCl, $MgCl_2$ and ASTM D1141 artificial seawater (ASW) and the corrosion response of mild steel surfaces contaminated with them.[7,8] We demonstrated that the DRH of these salts, both in singular form or as a mixture (ASW) did not serve as threshold between wet and dry and significant and insignificant corrosion. Furthermore, we observed that considerable electrolyte is present and corrosion can occur at humidity levels well below the DRH of $MgCl_2$ (33%) on steel contaminated with this salt or ASW.

The work presented here is an extension of this program, with specific focus on the relationship between the wetting and drying behavior of acidified ASW and the corrosion response of mild steel. Acidified ASW (pH ~3) is of interest as it more closely represents the acidic nature of SSA found in polluted coastal marine environments.[9] The aims of this study were to: (1) quantitatively characterize the relationship between solid-liquid phase transitions of acidified ASW microparticles and the corrosion response of steel contaminated with them in terms of RH, and (2) establish the RH and time frame under which there is sufficient electrolyte to cause corrosion. The understanding developed in this study along with results from our previous work are used to assess the accuracy and appropriateness of the time of wetness parameter for describing corrosion of SSA-contaminated surfaces.

To achieve these objectives, the hygroscopic behavior of acidified ASW microparticles deposited on an inert interdigitated electrode (IDE) sensor was characterized through impedance measurements. Additionally, the corrosion loss of mild steel contaminated with these microparticles and subjected to a range of isohumidity conditions was quantified using optical profilometry. Taken together, the results from the interdigitated sensor and steel coupon experiments clarify the relationship between the hygroscopic behavior of ASW and the corrosion response of steel.

EXPERIMENTAL PROCEDURE

Details of the experimental procedures are given in the following sections, but an overview is warranted here. Polished mild steel coupons were loaded with acidified artificial seawater droplets and subjected to isohumidity conditions ranging from <2% to 86% RH for periods of up to 30 days. After exposure, the samples were cleaned and surface profilometry was utilized to characterize attack morphology and quantify volume loss. The hygroscopic behavior of acidified ASW particles was studied using an IDE impedance sensing method.

Corrosion Exposures

Coupons of UNS G10100 plain carbon steel measuring 25 x 25 mm were polished to a 0.01 µm colloidal silica finish. After polishing, they were rinsed with ultrapure (UP) water (18.2 MΩ•cm, <5 ppb TOC) and absolute ethanol (>99.5%), then dried in a stream of zero grade compressed air.

Prior to exposure, aqueous droplets of ASTM D1141 artificial seawater acidified to a pH of 3.1 with HCl were dispensed onto each coupon using a custom inkjet printer in a 10 x 10 mm square array pattern using a method described elsewhere.[8,10] The in-air diameter of each droplet dispensed was ~35 µm, which is representative of the larger size fraction of natural SSA.[11] The resulting density of salt loaded onto each coupon was 16 $\mu g \cdot cm^{-2}$. These loadings, in terms of chloride content, are within the range of that measured on boldly exposed metal surfaces in coastal marine environments (10^{-1} to 10^{2} $\mu g \cdot cm^{-2}$ Cl^{-}).[12,13] Printing was carried out in ambient laboratory conditions, ~78% RH and 21 °C.

Immediately after printing, the coupons were placed in glass containers that contained saturated salt solutions or desiccant to maintain a particular RH. Two to four coupons were placed in a chamber at each set point. In order to ensure the droplets remained largely wet (deliquesced) at the start of the isohumidity exposures, the containers were prefilled with humidified zero air to achieve 70-80% RH prior to closing. After filling with humidified air, the air ports on the chambers were closed and they were left to equilibrate to the RH set point governed by the salt solution or desiccant at 21±2 °C. The chambers were monitored with a calibrated RH meter (±1.5% accuracy) which indicated that the atmospheres in the chambers equilibrated to within 2% of the expected RH set point in less than one hour. Coupons were removed at 12 hour, 1 day, 7 day and 30 day intervals.

After exposure, samples were immediately stripped of rust and scanned using an optical profilometer. Rust removal consisted of immersing the coupons in an aqueous diammonium citrate solution at 40 °C for 1-5 min followed by rinsing in UP water and drying in a stream of zero air. The cleaned coupons were scanned using a calibrated white light profilometer. The manufacturer-stated height resolution of the instrument in the configuration used was 1 nm with a lateral resolution of 500 nm. At least three 1 x 1 mm areas of each coupon within the printed (salt deposited) area and one 1 x 1 mm area outside the printed area were scanned. Each scan was then analyzed to determine total volume loss and maximum pit depth with respect to the original polished plane of the coupon.

Hygroscopic Behavior of ASW on Sensor

The hygroscopic behavior of ASW was investigated using an IDE impedance sensing method along with time-lapse optical microscopy.[14] Droplets of the acidified seawater solution used for the corrosion exposures were deposited onto an IDE sensor inside the inkjet printer. The sensor consisted of a pair of interdigitated platinum electrodes arranged in a comb pattern on a fused quartz substrate. Spacing between the electrodes was 3 μm. After depositing the droplets, the droplet-loaded sensor was left inside the inkjet printer chamber and subjected to cyclic humidity ramping at 21±2 °C. Dry compressed air flowed through the printer chamber at 8 L/min to create a slight positive pressure with respect to the laboratory. Prior to entering the chamber the compressed air was filtered through activated carbon and 4 Å molecular sieves and then passed through a 0.2 μm particulate filter to remove trace contaminants and water vapor. Humidity inside the chamber was controlled and logged using a programmable humidity control system, which was comprised of a PID controller, a calibrated RH sensor and a recirculating air ultrasonic humidifier filled with UP water. The RH sensor had a calibrated accuracy of ±1.5% RH under the exposure conditions of this study.

Impedance was measured at 0.2 Hz and 26 kHz across the sensors using a potentiostat in a two-electrode. The higher frequency was used because it was most indicative of bulk phase transitions and is one of the highest frequencies that did not exhibit instrument artifacts. The lower frequency was chosen because it was most sensitive to the presence of small amounts of electrolyte while still providing a reasonable sampling time. An excitation voltage of 20 mV versus open circuit was used. Measurements were taken at four minute intervals during the humidity ramping experiments. Measurements were also normalized to remove the admittance contribution of the sensor and noise from the experimental setup. Thus, a normalized measured value below unity indicates that admittance is contributed from the hygroscopic particles on the sensor alone. The deposited particles were also monitored via a variable zoom optical microscope. The microscope was trained on the sensing area during the humidity ramping experiments and images taken at four minute intervals. Further details on this method and the instrumentation utilized are described elsewhere.[14]

RESULTS

Humidity Cycling of Salt-Loaded IDE Sensor

Measurements during humidity cycling of the acidified ASW-loaded sensor indicate five major sharp transitions in particle coverage and impedance and show significant admittance due to particle presence throughout the experiments. The measured RH profile and impedance during one of the three replicate humidity cycles carried out is given in Figure 1. Impedance measured at 26 kHz is recast as a function of RH in Figure 2. Inset in Figure 2 are images taken during or after major shifts in

impedance. The shifts in impedance were found to correspond with visual changes of the particles. At the start of the experiment, particles were in the form of droplets containing small crystals, Figure 2(a). They stayed in this configuration until rapidly shrinking at 50% RH (b). What appeared to be liquid was still present around these shrunken deposits until another shrinking event occurred at 11% RH, prior to (c). Below 11% RH and up to the onset of the humidification ramp the impedance at both frequencies gradually rose, Figures 1 and 2(c). Impedance at 0.2 Hz remained significantly below unity throughout, Figure 1, indicating admittance contribution from the presence of the particles. At the onset of humidification, impedance at 0.2 Hz dropped followed by 26 kHz when RH reached 10%. This correlated with small growth in particle size Figure 2 (d). A drop in impedance again occurred around 30% RH corresponding to visual appearance of a liquid-like layer around the particles (e). The particles then gradually grew in size until a major deliquescence event took place at 75% RH (f) causing the deposits to revert back to their state at the start of the experiment. The morphological changes and impedance behavior described above were nearly identical for all three humidity cycles.

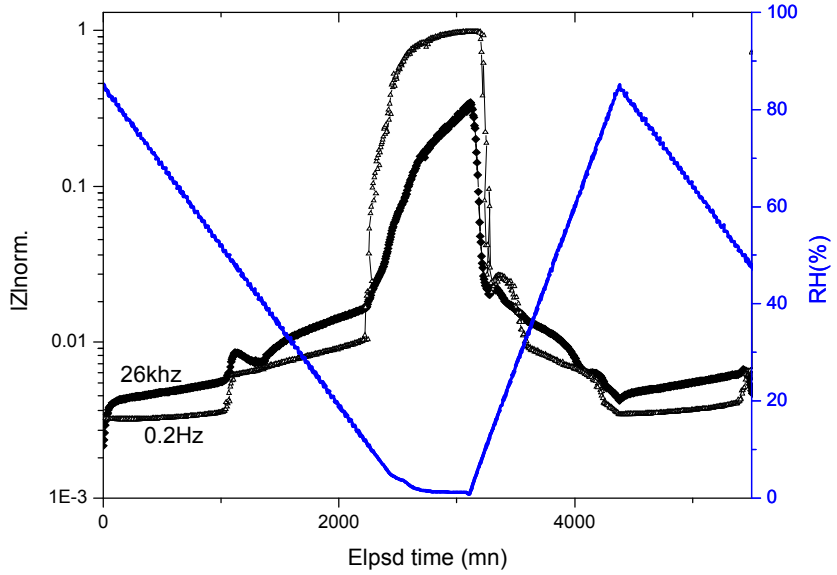

Figure 1: Impedance measured across an IDE sensor loaded with acidified ASW at two frequencies during a humidity cycle.

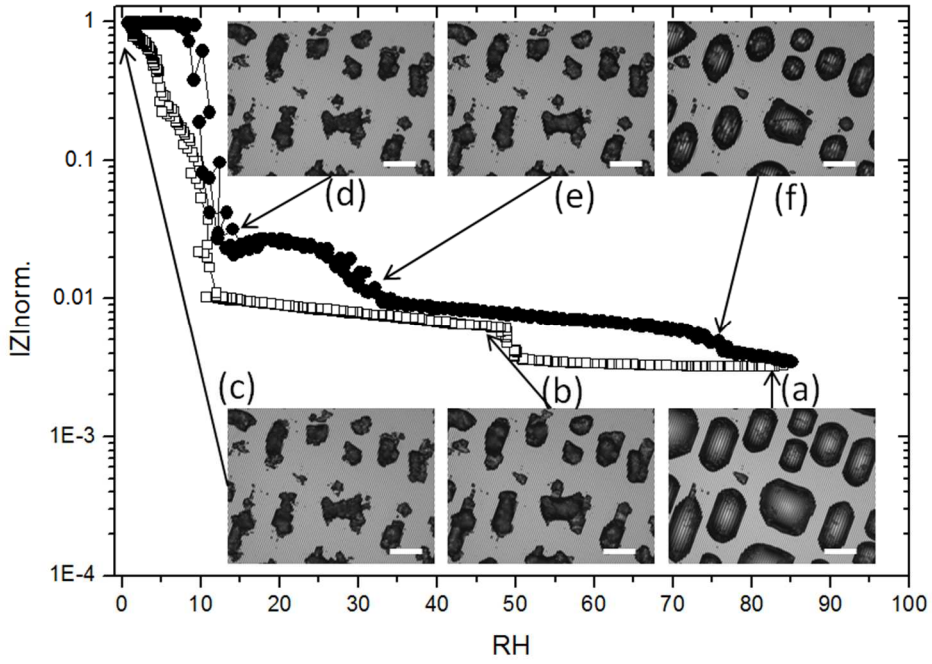

Figure 2: Impedance measurements at 26 kHz, from Figure 1, recast as a function of RH along with optical micrographs of the particles on the sensor surface during various points of the humidity cycle. The open symbols are measurements taken during dehumidification and the closed symbols were taken during humidification. The scale bar in the images is 100 µm.

Corrosion of Steel Coupons

Isohumidity exposures of acidified ASW on steel indicated that sustained corrosion occurred down to at least 11% RH and attack became more severe with increasing RH and time. Figure 3 exhibits the mean nominal corrosion depth (volume loss/scan area) measured on the salt loaded steel coupons. Corrosion depth appears significantly different at 11% RH for the 30 day samples with respect to the 11% RH exposures at lesser durations, indicating that loss became resolvable after 7 days. Average loss was highest at ≥ 64% RH at greater than 7 days, but also appears to flatten out with respect to RH above this threshold. The average maximum pit depth, Figure 4, generally increased with increasing time and RH as well. It is interesting to note, however, that increases in pit depth with time were relatively small or unresolvable with respect to measurement uncertainty at ≤ 33% RH. This was despite the fact that volume loss was observed to increase at ≤ 33% RH. This appears to be a reflection of the fact that corrosion attack was visually observed to occur in the form of radial spreading of shallow pitting from the salt deposits over time in this humidity range.

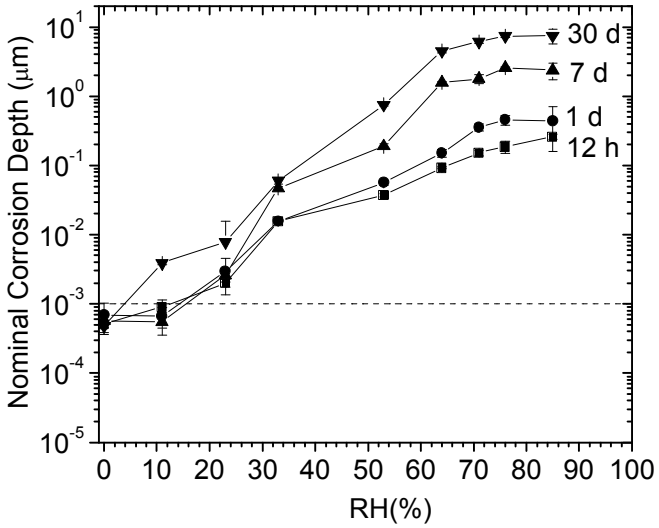

Figure 3: Average volume loss divided by scan area (nominal depth) for acidified ASW-loaded coupons exposed to a range of isohumidity conditions. The bars represent one standard deviation. The dashed line is the upper bound of the 95% confidence interval of volume loss measured on clean areas outside the printed salt pattern.

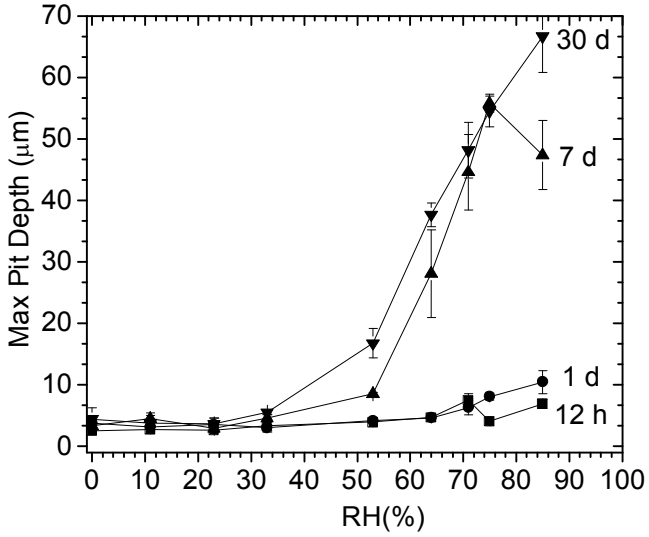

Figure 4: Average maximum pit depth measured on coupons loaded with acidified ASW and exposed to a range of isohumidity conditions. The bars represent one standard deviation.

DISCUSSION

Hygroscopic Behavior of Acidified ASW

The results of the salt on sensor experiments indicate that varying amounts of electrolyte were associated with the salt deposits during the entirety of the exposures. The major liquid-solid transitions of the sensor-deposited acidified ASW particles during humidity cycling with respect to RH are similar to that exhibited by non-acidified ASW particles examined in previous work.[7] In our previous work, these transitions were associated with NaCl and $MgCl_2$, the two primary constituents of artificial seawater (and natural seawater) by mass. It is reasonable to attribute the transitions observed for acidified seawater to these constituents as well. The large transitions at ~50% RH during dehumidification and 76% RH during humidification, Figure 2, are characteristic of the efflorescence and deliquescence behavior of both pure NaCl, as well as NaCl in synthetic and natural sea salt.[7] It is possible that analogous transitions near 10% RH, in Figure 2, as was also seen for non-acidified ASW, are due to the behavior of a metastable magnesium chloride hydrate salt. One exception to the similarity between the non-acidified results previously reported and the results presented here is that the acidified ASW additionally exhibited impedance transitions around 33% RH, which may be due to the presence of resolvable amounts of the thermodynamically predicted $MgCl_2.6H_2O$.

Although major phase transitions occurred down to 9% RH during dehumidification, the ASW particles retained significant conductance even after holding for 24 h at <2% RH, which may be indicative of the presence of some form of electrolyte. The low humidity admittance is most evident in the $|Z|_{0.2Hz}$ curve in Figure 1, which remains significantly below that measured across a clean, unloaded sensor (unity value of normalized impedance). The continual rise in $|Z|_{0.2Hz}$ when the RH was held constant at <2% RH and its movement in step with RH immediately upon subsequent humidification demonstrates that this admittance is governed by water availability, Figure 1. This behavior, again, was seen for deposits of ASW and for pure $MgCl_2$ in our previous work.[7,14] In the case of pure $MgCl_2$ deposits, we found the slowly rising impedance measured upon holding at <2% RH reflected the evaporation of fluid trapped under partially effloresced deposits.[14] The fluid trapping occurred due to the formation of solid shells at the electrolyte-air interface of the drops during efflorescence. Given the apparent controlling behavior of $MgCl_2$ on non-acidified ASW particle conductance at low humidity in previous work, we proposed that similar fluid trapping also occurred with ASW. It is likely that such behavior may occur for acidified ASW as well.

Effect of RH on Corrosion Response

Consistent with the observation that electrolyte may be present down to at least 2% RH at room temperature under the acidified ASW salt deposits, the 30 d volume loss results indicate that the minimum RH at which sustained corrosion was detectable was 11% RH, Figure 3. The corrosion rates at these levels, however, are relatively trivial, as exemplified in Figure 5. In this figure, the 12 h volume loss data have been subtracted from the 30 d data, both shown in Figure 1, and the result was normalized to a per annum corrosion rate. This eliminates the high rate of corrosion that occurred upon initial loading of the salt droplets onto the coupons at high humidity (~80% RH) at the start of the experiments. Also shown in this figure are the results from a previous set of experiments[7] carried out in the same manner except using as-is ASTM seawater (pH = 8.2).

From Figure 5, it is evident that both acidified and normal ASTM artificial seawater invoke similar corrosion rate trends with respect to RH. Acidification of ASTM seawater created a more aggressive solution that resulted in relatively higher corrosion rates. These results suggest that acidification seems to have a lasting effect on corrosion rate, despite the expected drastic changes in solution chemistry (including pH) that occurs at the anode and cathode sites due to corrosion and interaction with the surrounding atmosphere. It is notable here that, unlike the acidified seawater, the corrosion rates measured for ASW at 33% RH were below the limits of detection. In our previous work, however, we had shown that higher salt loading densities (100x) allowed for detection of sustained corrosion below

33% RH. In other words, corrosion was likely occurring but at rates lower than the detection limits of our technique.

A large inflection in corrosion loss trends with respect to RH for the acidified ASW loaded coupons for longer times initiated between 33% and 53% RH, which is not directly relatable to the phase transitions observed on the impedance sensor nor predicted for seawater, and similar to that of non-acidified ASW, Figure 6. These observations are in agreement with those of Evans and Taylor and Duly who also reported corrosion to become considerable within this range for natural sea salt contaminated carbon steel, based on results of similar isohumidity experiments.[15,16] The cause of this general behavior remains an area for further study.

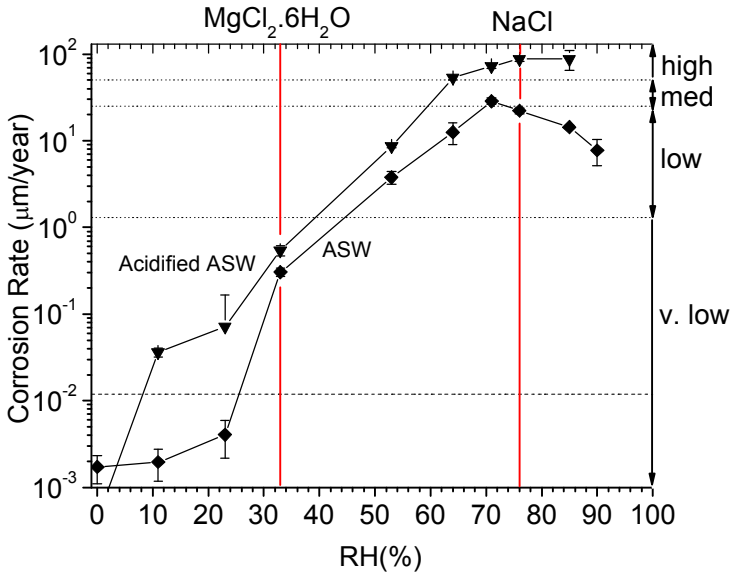

Figure 5: 30 day volume loss data from acidified and non-acidified[7] ASW-loaded coupons (with same salt loading density) normalized to a per annum corrosion rate and compared to the DRH of NaCl (76%) and $MgCl_2.6H_2O$ (33%) along with the ISO 9223 atmospheric corrosivity classifications for steel. The lowest dashed line represents the upper bound of the 95% confidence interval of volume loss measured on clean areas outside the printed salt pattern. The bars represent one standard deviation.

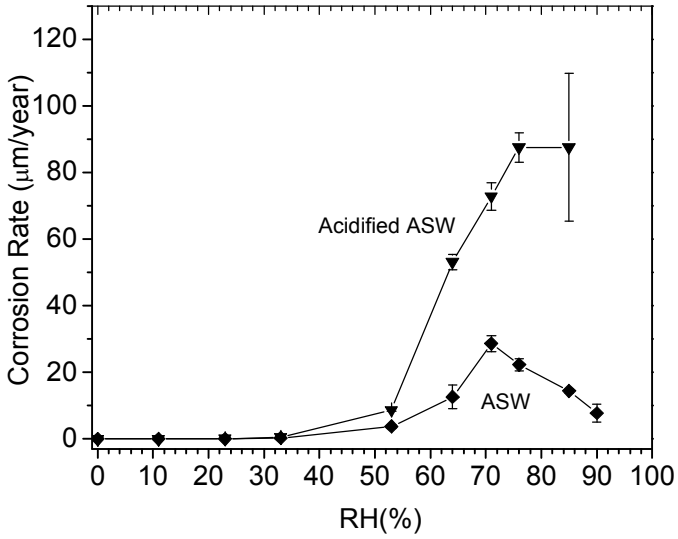

Figure 6: Comparison of acidified and non-acidified[7] ASW corrosion rates from Figure 5 recast on a linear scale.

Implications for TOW

These results raise the question as to whether surfaces contaminated with SSA ever truly dry in natural ambient conditions (in terms of corrosion being possible). Major liquid-solid phase transitions of ASW occurred at ~10% RH, attributed to a metastable hydrated Mg-Cl phase, and the ASW deposits remained significantly conductive down to <2% RH, even for 24 hours, likely due to fluid trapping. Such low RH conditions are rarely encountered in ambient natural environments.[17] They could, however, be encountered on heated surfaces , such as those receiving direct solar exposure, where the surface RH can be much lower than that of the ambient environment. Surface heating was not addressed in the room temperature experiments reported here, nor was the effect of temperature on the hygroscopic behavior of ASW. Further work is needed to examine the effect of heating on the hygroscopic behavior of SSA proxies, and, importantly, natural SSA to provide a more conclusive answer to this issue.

Regardless of whether a surface ever truly dries, our findings challenge the commonly utilized humidity based thresholds for estimations of TOW on SSA contaminated surfaces. These include the ISO 9223 threshold of 80% RH and use of the DRH of sea salt components, including that of $MgCl_2.6H_2O$ (33%).[13,18,19] In previous work, we demonstrated that corrosion can initiate by adsorbed water on NaCl crystals down to 33%RH, and proceed at rates comparable to that at and above the DRH of NaCl (76%) at humidity levels down to 53% due to development of hygroscopic corrosion chemistry.[8] Here we found corrosion can be sustained down to at least 11% RH, possibly due to trapped fluid or deliquesced electrolyte Mg-Cl rich electrolyte, which is well below the DRH of $MgCl_2.6H_2O$ (33%). No substantial inflection in the trends of corrosion loss as a function of RH were notable at the observed or predicted phase transitions in any of these cases. Considering that these deliquescence points proved relatively insignificant under simple sea salt proxies in highly controlled conditions, it is doubtful that such delineation will be witnessed in the natural environment where surface chemistry and RH-T transients are much more complex.

CONCLUSIONS

The hygroscopic behavior of acidified artificial seawater particles was characterized and linked to the humidity-induced corrosion response of mild steel contaminated with them. The following conclusions were drawn:

1. Humidity cycling of acidified ASTM artificial seawater microparticles on an interdigitated electrode sensor indicated liquid-solid phase transitions occurred at ~10% RH, with evidence of significant conductance down to <2%, even after 24 h. This behavior was found to be nearly identical to that of non-acidified seawater in previous work. The low humidity behavior seen for the acidified seawater is postulated to be due to the formation of metastable $MgCl_2$ hydrates and fluid trapping under a solid salt crust.

2. Trends in corrosion loss versus RH were not directly reflective of the major liquid-solid phase transitions observed during humidity cycling of the acidified ASW alone nor of the predicted deliquescence points of its major constituents. The minimum RH where sustained corrosion was detectable was 11%. Trends observed for acidified ASW-loaded steel generally followed those of non-acidified ASW-loaded steel.

3. Further work is suggested to test the universality of these findings in cases of varying salt loadings, more complex chemistries, diurnal humidity and temperature transients, and exposure times more representative of surfaces exposed to outdoor conditions. The experimental framework developed here serves as one means of doing so.

ACKNOWLEDGEMENTS

This work has been supported by the US Air Force Academy under agreement FA8501-UVA-002. Daniel J. Dunmire, Director, DoD Corrosion Policy and Oversight, OUSD (AT&L), Office of the Secretary of Defense and the SERDP/ESTCP program via contract W912HQ-09-C-0042 are also gratefully acknowledged. Sandia National Laboratories is a multi-program laboratory managed and operated by Sandia Corporation, a wholly owned subsidiary of Lockheed Martin Company, for the United States Department of Energy's National Nuclear Security Administration under Contract DE-AC04-94AL85000

REFERENCES

1. Cole, I. S.; Ganther, W. D.; Sinclair, J. D.; Lau, D.; Paterson, D. A., A study of the wetting of metal surfaces in order to understand the processes controlling atmospheric corrosion. *J. Electrochem. Soc.* **2004,** *151* (12), B627-B635.
2. Schindelholz, E.; Kelly, R. G.; Cole, I. S.; Ganther, W. D.; Muster, T. H., Comparability and accuracy of time of wetness sensing methods relevant for atmospheric corrosion. *Corros. Sci.* **2013,** *67*, 233-241.
3. Roberge, P. R., Atmospheric Corrosion. In *Uhlig's Corrosion Handbook*, 3 ed.; Revie, R., Ed. John Wiley & Sons: Hoboken, New Jersey, 2011; pp 299-327.
4. Nishikata, A.; Tsutsumi, Y.; Tsuru, T., Corrosion monitoring of stainless steels in marine atmospheric environment. In *Corrosion and Electrochemistry of Advanced Materials*, Fujimoto, S.; Akiyama, E.; Habazaki, H., Eds. Electrochemical Society: Los Angeles, CA, United states, 2005; p 652.
5. Schindelholz, E.; Kelly, R. G., Wetting phenomena and time of wetness in atmospheric corrosion: a review. *Corros. Rev.* **2012,** *30* (5-6), 135-207.
6. Noda, K.; Yamamoto, M.; Masuda, H.; Kodama, T. In *atmospheric corrosion process of ferritic alloy under seashore environment* Corrosion and Corrosion Control in Saltwater Environments: Proceedings of the International Symposium, The Electrochemical Society: 2000; p 144.
7. Schindelholz, E.; Risteen, B.; Kelly, R., Effect of relative humidity on corrosion of steel under sea salt aerosol proxies II. $MgCl_2$, artificial seawater. *J. Electrochem. Soc.* **2014,** *161* (10), C460-C470.
8. Schindelholz, E.; Risteen, B.; Kelly, R., Effect of relative humidity on corrosion of steel under sea salt aerosol proxies I. NaCl. *J. Electrochem. Soc.* **2014,** *161* (10), C450-C459.
9. Keene, W. C.; Savoie, D. L., The pH of deliquesced sea-salt aerosol in polluted marine air. *Geophysical Research Letters* **1998,** *25* (12), 2181-2184.
10. ASTM, ASTM Standard D1141. In *Standard Practice for the Preperation of Substitute Ocean Water*, ASTM International: West Conshohocken, PA, 2013.

11. O'Dowd, C.; de Leeuw, G., Marine aerosol production: a review of the current knowledge. *Philosophical Transactions of the Royal Society A: Mathematical, Physical and Engineering Sciences* **2007,** *365* (1856), 1753-1774.
12. Shinohara, T.; Motoda, S.-I.; Oshikawa, W., Evaluation of corrosivity of atmosphere by ACM type corrosion sensor. *Zairyo to Kankyo/ Corrosion Engineering* **2005,** *54* (8), 375-382.
13. Cole, I. S.; Ganther, W. D.; Lau, D., Field studies of surface cleaning and salt retention on openly exposed metal plates. *Corros. Eng. Sci. Technol.* **2006,** *41* (4), 310-20.
14. Schindelholz, E.; Tsui, L.-k.; Kelly, R. G., Hygroscopic particle behavior studied by interdigitated array microelectrode impedance sensors. *J. Phys. Chem. A* **2013,** *118* (1), 167-177.
15. Evans, U. R.; Taylor, C. A. J., Critical humidity for rusting in the presence of sea salt. *Br. Corros. J.* **1974,** *9* (1), 26-28.
16. Duly, S., The corrosion of steel by sea salt of given moisture content. *Journal of the Society of Chemical Industry* **1950,** *69* (10), 304-306.
17. Stewart, D. A. *Low Relative Humidity in the Atmosphere*; TK-RD-RE-89-3; U.S. Army Missile Command: Redstone Aresenal, Alabama, 1989; p 55.
18. ISO, 9223:1992(E) Corrosion of metals and alloys- Corrosivity of atmospheres- Classification. ISO: Geneva, Switzerland, 1992; Vol. ISO 9223:1992(E).
19. Ganther, W. D.; Cole, I. S.; Helal, A. M.; Chan, W.; Paterson, D. A.; Trinidad, G.; Corrigan, P.; Mohamed, R.; Sabah, N.; Al-Mazrouei, A., Towards the development of a corrosion map for Abu Dhabi. *Mater. Corros.* **2010**, 1066-1073.